

Muography in Colombia: Simulation Framework, Instrumentation, and Data Analysis

J. Peña-Rodríguez,¹ A. Vesga-Ramírez,² A. Vásquez-Ramírez,¹ M. Suárez-Durán,³ R. de León-Barrios,¹
D. Sierra-Porta,⁴ R. Calderón-Ardila,⁵ J. Pisco-Guavabe,¹ H. Asorey,^{5,6}
J. D. Sanabria-Gómez,¹ and L. A. Núñez^{1,7}

¹*Escuela de Física, Universidad Industrial de Santander, Bucaramanga, Colombia*

²*International Center for Earth Sciences, Comisión Nacional de Energía Atómica, Buenos Aires, Argentina*

³*Université Libre de Bruxelles, Bruxelles, Belgium*

⁴*Facultad de Ciencias Básicas, Universidad Tecnológica de Bolívar, Cartagena de Indias, Colombia*

⁵*Instituto de Tecnologías en Detección y Astropartículas, Centro Atómico Constituyentes, Buenos Aires, Argentina*

⁶*Consejo Nacional de Investigaciones Científicas y Técnicas, Buenos Aires, Argentina*

⁷*Departamento de Física, Facultad de Ciencias, Universidad de Los Andes, Mérida, Venezuela*

Corresponding author: J. Peña-Rodríguez

Email: jesus.pena@correo.uis.edu.co

Abstract

We present the Colombo-Argentinian Muography Program for studying inland Latin American volcanoes. It describes the implementation of a simulation framework covering various factors with different spatial and time scales: the geomagnetic effects at a particular geographic point, the development of extensive air showers in the atmosphere, the propagation through the scanned structure, and the detector response. Next, we sketch the criteria adopted for designing, building, and commissioning *MuTe*: a hybrid Muon Telescope based on a composite detection technique. It combines a hodoscope for particle tracking and a water Cherenkov detector to enhance the muon-to-background-signal separation due to extensive air showers' soft and multiple-particle components. *MuTe* also discriminates inverse-trajectory and low-momentum muons by using a picosecond Time-of-Flight system. We also characterize the instrument's structural—mechanical and thermal—behavior, discussing preliminary results from the background composition and the telescope-health monitoring variables. Finally, we discuss the implementations of an optimization algorithm to improve the volcano internal density distribution estimation and machine learning techniques for background rejection.

Keywords: muon tomography, muon telescope, simulation framework, instrumentation, data analysis

DOI: 10.31526/JAIS.2022.271

1. VOLCANOES IN LATIN AMERICA AND COLOMBIA

Latin America is part of the Pacific Ring of Fire, with more than 200 Holocene volcanoes sculpting the Andean mountain range traversing the continent. Almost 20 million people live close to active volcanic zones (<100 km). Four geographic areas group volcanoes in South America: Northern, Central, Southern, and Austral, with more than 600 eruptions reported since 1532, causing 25000 casualties. The most deadly was the disaster that occurred with the lahars of the Nevado del Ruiz (23000 deaths), Colombia, in 1985 [1].

Volcanoes cause ash clouds, eruptions, pyroclastic flows, lahars, debris avalanches, and earthquakes. The previous monitoring of related phenomena allows the prevention of disasters and casualties. Information on seisms, ground deformation, gas emissions, and thermal anomalies helps to alert authorities and citizens about possible hazards. About 60% of Andean volcanoes remain unmonitored due to a lack of resources, remote access, and dangerous conditions for the installations of equipment locally [2].

Colombia has more than a dozen active volcanoes (Azufra, Cerro Negro, Chiles, Cumbal, Doña Juana, Galeras, Machín, Nevado del Huila, Nevado del Ruiz, Nevado Santa Isabel, Nevado del Tolima, Puracé, and Sotará) clustered in three main groups along the Cordillera Central, the highest of the three branches of the Colombian Andes. Most of these volcanoes represent a significant risk to the nearby population in towns and/or cities [3, 4, 5].

The Galeras, Cerro Machín, and Nevado del Ruiz volcanoes represent a high risk for Colombian citizens. Evidence of that was the Nevado del Ruiz eruption on November 13, 1985, which involved the partial melting of the glacier cap and consequent lahars. Mood flows reached the municipality of Armero-Tolima, causing more than 23000 casualties [6].

The Cerro Machín volcano, with a crater of 2.4 km diameter and 450 m height, could cause a future pyroclastic eruptive episode reaching an area of 10 km² around the volcano edifice [7]. The similarities in morphologies between two volcanoes must be con-

sidered in the risk evaluation of an eventual eruption. The Machín¹ volcano has a morphology similar to the Chichón/Chichonal² volcano in southern state of Chiapas in México [6]. The Chichón has been the most deadly eruption in Mexico, creating an ash cloud covering 200 km, ~2000 casualties, and the displacement of ~20000 citizens in March 1982 [8].

2. MUOGRAPHY IN THE LATIN AMERICAN REGION

Muography is a non-invasive technique for scanning the inner structure of volcanoes. This method uses the attenuation of atmospheric muons after crossing the volcanic edifice. The emerging muon flux measurements in different directions give estimations for the density distributions of volcanic edifices [6].

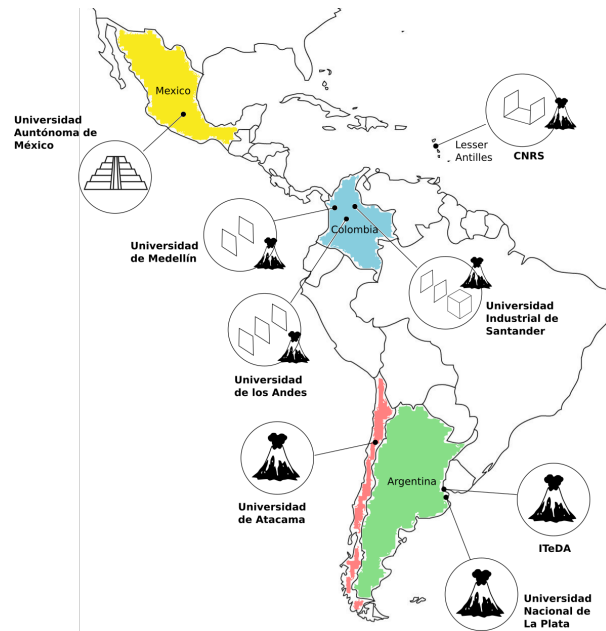


FIGURE 1: Geographical distribution of universities/institutions actively working in muography in Latin America. Most of them are focused on muography applied to vulcanology. Argentina and Colombia register most activities with groups cooperating in different areas.

Several Latin American universities/institutions (see Figure 1) work in muography due to the number of active volcanoes along the Andean mountain range and the risk they represent. The Latin American muography consists of three research areas: creation of simulation frameworks, development of instrumentation, and implementation of data analysis methods [9, 10].

Muography simulation tools and frameworks estimate the atmospheric muon flux [11, 12], muon propagation through the geological target [6, 13, 14], detector response [15, 16, 17], and density optimization [18] by using Monte Carlo codes. The development of muography instruments has been addressed from different perspectives: the use of continuous scintillators [16], scintillators strips [19], hybrid muon telescopes for enhancing the muon-to-background ratio [20, 21], and the development of new technologies [22].

The Muon Telescope implements machine learning algorithms for particle identification of signal/background using the deposited energy, time of flight, and momentum [23]. Muography brings data analysis challenges from raw data treatment to solving the density estimation inverse problem. Simulated annealing and Bayesian dual inversion algorithms tackle the inverse problem to infer the target density distribution [18, 24].

3. THE MUON TELESCOPE

The Muon Telescope (MuTe) project³ involves designing and implementing a muon detector for scanning volcanoes. The project boosts the muography research area in Colombia in close collaboration with Argentinian colleagues, providing an innovation ecosystem between the two countries. This R&D area identifies three lines of action: the simulation framework, the instrumentation, and online/offline data analysis. The simulation framework implements Monte Carlo simulations to estimate the muon flux at any geographical point and then estimate the energy loss of the crossing muons and the detector response. The instrumentation

¹https://es.wikipedia.org/wiki/Cerro_Machin

²<https://en.wikipedia.org/wiki/Chichonal>

³<https://halley.uis.edu.co/fuego>

branch manages the steps of designing, implementing, and calibrating the Muon Telescope. The data analysis branch processes the recorded data and develops algorithms for background rejection and density inverse problem-solving.

The MuTe combines two detection techniques as shown in Figure 2. A hodoscope measures the muon flux by tracking the particle trajectories and a water Cherenkov detector (WCD) which records the deposited energy of particles traversing the MuTe. A time-difference system for the hodoscope measures the time of flight of particles impinging the detector [20]. The particle identification system of MuTe allows the rejection of muography background sources: the soft component of Extended Air Showers, backscattering particles, and forward scattering muons [23].

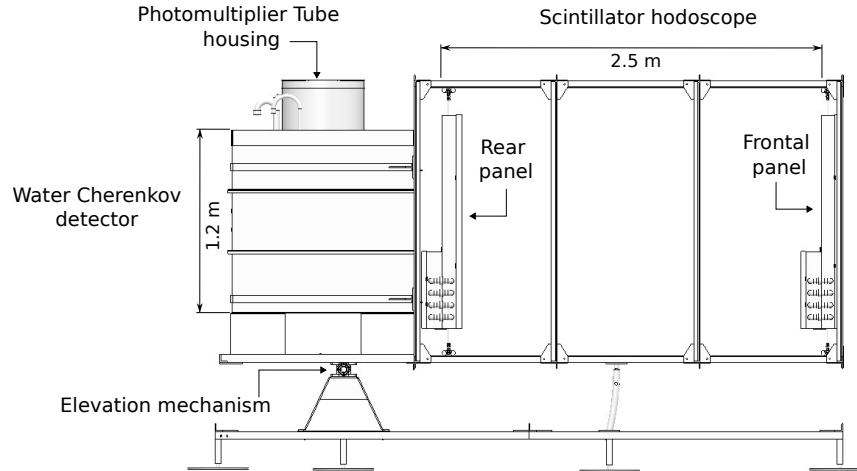


FIGURE 2: MuTe lateral view. The WCD, placed behind the scintillator hodoscope, measures the deposited energy of particles traversing the MuTe. The hodoscope measures the time of flight and reconstructs the trajectory of the impinging particles. The separation distance between the hodoscope panels varies from 40 cm up to 250 cm.

A photovoltaic system supplies the MuTe with autonomy for up to 6 days in cloudy conditions. The MuTe daily reports the hodoscope and WCD status: power consumption, average particle flux, detector temperature, atmospheric pressure, and environmental humidity.

4. SIMULATION FRAMEWORK

As shown in Figure 3, the simulation scheme for the MuTe project implements the ARTI framework from the Latin American Giant Observatory collaboration. This framework considers three essential factors with different spatial and time scales: the geomagnetic effects, the development of the extensive air showers in the atmosphere, and the detector response at ground level [15, 25, 26].

In the first step, a MAGNETOCOSMICS⁴-based script computes the primary cosmic ray flux impinging the Earth's atmosphere after modulation due to the geomagnetic field rigidity. Then, a second step uses the CORSIKA⁵ script that simulates the interaction of primary cosmic rays and the Earth's atmosphere. We compute the spectrum of atmospheric particles reaching the observation place and the angular (zenith and azimuth) dependency of the muon flux [27]. We found secondary cosmic rays at Cerro Machín volcano (4°29'00"N, 75°23'30"W, 2749 m a.s.l.) to be mainly composed of electromagnetic particles (photons, electrons, and positrons) and muons.

MUSIC-MUSUN codes [28, 29] and Python/MATLAB scripts calculate the ray tracing, the volcano opacity, the muon energy loss, and the emerging muon flux and estimate the period of observation [6, 30, 27]. The code obtains the volcano topography from the SRTM⁶ NASA database. The energy loss is calculated considering losses by ionization and Bremsstrahlung through a standard rock density ($\rho = 2.65 \text{ g/cm}^3$) or any particular rock compositions in the case of MUSIC-MUSUN codes.

We use GEANT4 in two steps of the simulation framework: by estimating the muon forward scattering effect and assessing the MuTe detector response. In the first case, we evaluated the angular deviation of muons (0–10 GeV/c energy and 0–90° zenith angle) after interacting with a standard rock surface. We concluded that the muon forward scattering effect is negligible ($<1^\circ$ for muon momenta above 5 GeV/c and incident zenith angles smaller than 85° in relation to the surface's normal [20]).

In the second case, the script estimated the deposited energy spectrum of particles impinging the WCD, the photoelectron spectrum of the scintillator strips, and the panel attenuation. We found that a vertical muon deposits $\sim 240 \text{ MeV}$ in the WCD, and losses $\sim 2.08 \text{ MeV}$ in the scintillator strip generating an average signal of 40 photo-electrons. This signal attenuates up to 12% in the panel corner opposite to the SiPM location [15]. Optical parameters (solid angle and acceptance) of MuTe were also computed. MuTe can reconstruct 3481 trajectories with a maximum acceptance of $3.69 \text{ cm}^2 \text{ sr}$ [31, 6].

⁴<http://cosray.unibe.ch/~laurent/magnetocosmics/>

⁵<https://www.iap.kit.edu/corsika/>

⁶<https://www2.jpl.nasa.gov/srtm/>

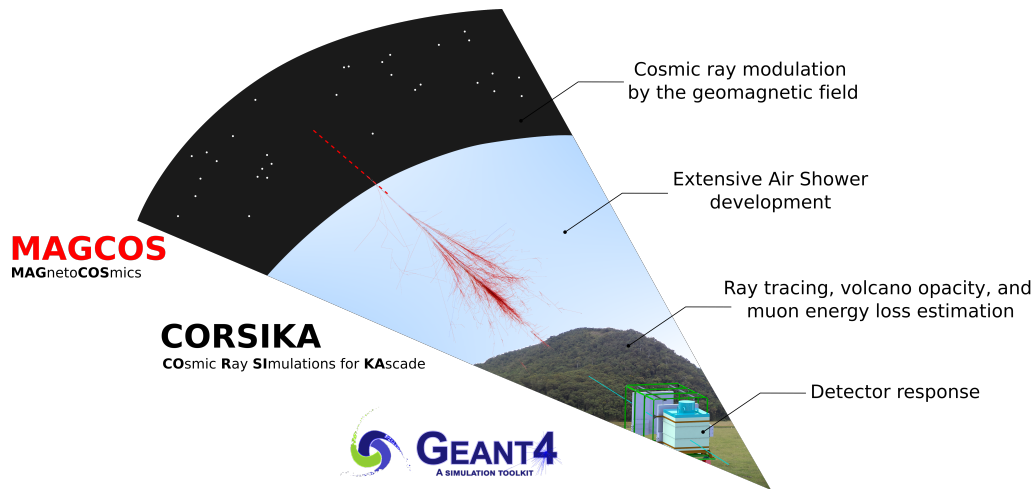


FIGURE 3: Muography simulation framework. MAGCOS computes the cosmic ray modulation due to the geomagnetic field, and CORSIKA estimates the atmospheric particle flux at the observation place. MUSIC, Python, and MATLAB scripts compute the ray tracing, volcano opacity, and emerging muon flux (considering energy loss and scattering). GEANT4 simulates the detector response.

5. INSTRUMENTATION

MuTe combines a scintillator hodoscope and a water Cherenkov detector. The hodoscope is based on independent modules made of 30 scintillators bar per panel ($120\text{ cm} \times 4\text{ cm} \times 1\text{ cm}$), a WLS fiber (Saint-Gobain BCF-92), a SiPM (Hamamatsu S13360-1350CS), and the electronics frontend. An RG-174U coaxial cable transmits the SiPM pulses to the acquisition system. The SiPM electronics frontend and the scintillator panel assembly are shown in Figure 4.

Two MAROC3A ASICs perform the gain-tuning and discrimination of the 120 scintillator signals. A couple of Cyclone III FPGAs configure the DAQ slow control parameters.

We established a discrimination threshold of 8 photo-electrons considering the SiPM noise analysis. The MuTe controls the SiPMs bias voltage using a programmable power supply (Hamamatsu C11204).

MuTe datasets combine particle flux and environmental data (temperature, barometric pressure, and power consumption) for postprocessing, detector status monitoring, and calibration procedures. A GPS pulse-per-second signal synchronizes the hodoscope and WCD data.

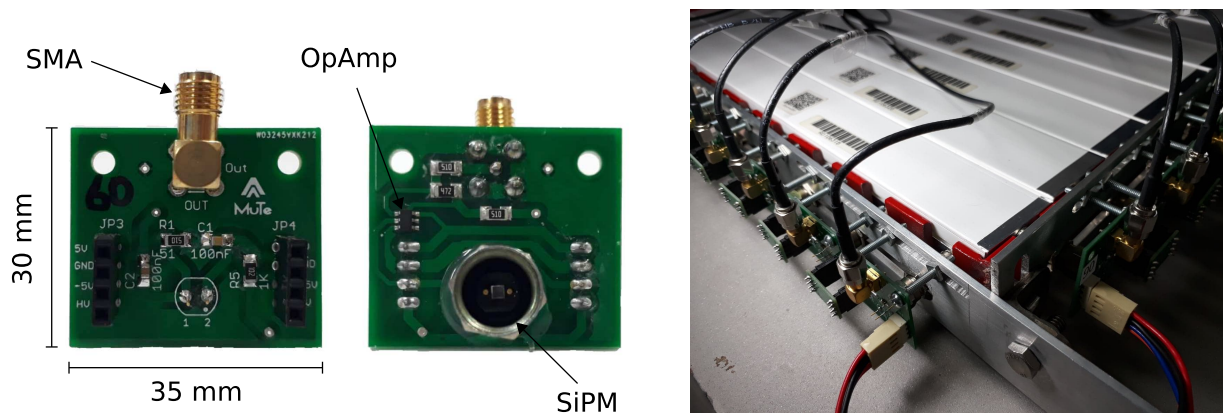


FIGURE 4: (Left) SiPM electronics frontend. (Right) Mechanical assembly of the scintillator bar, the Saint-Gobain BCF-92 WLS fiber, the Hamamatsu S13360-1350CS SiPM, and the transmission cables (coaxial RG-174U).

A PMT (photomultiplier tube Hamamatsu R5912) detects the Cherenkov light from the charged particles crossing the WCD. A high-voltage power supply EMCOC20 biases the PMT from 0 to 2000 V. Two 10-bit ADCs digitize the PMT anode and last-dynode signals at a frequency of 40 MHz. An FPGA Nexys II handles the tasks of thresholding, base-line correction, temporal labeling, and temperature-pressure recording.

The third ADC channel in the WCD digitizes a NIM signal from the hodoscope indicating a double coincidence event (hodoscope + WCD). A Cubieboard-2 sets the acquisition parameters (discrimination thresholds and the PMT bias voltage) of the WCD [20, 31].

During the development of the MuTe project, we implemented several specialized equipment and instrumentation for muography. We designed a controlled environment for the calibration of Silicon Photomultipliers (see Figure 5). This equipment allows us to control the SiPM temperature, bias voltage, and pulsed-light stimulus. We characterized the SiPM parameters as breakdown voltage, gain, dark count, afterpulsing, and crosstalk, and their dependency on temperature [32, 33].

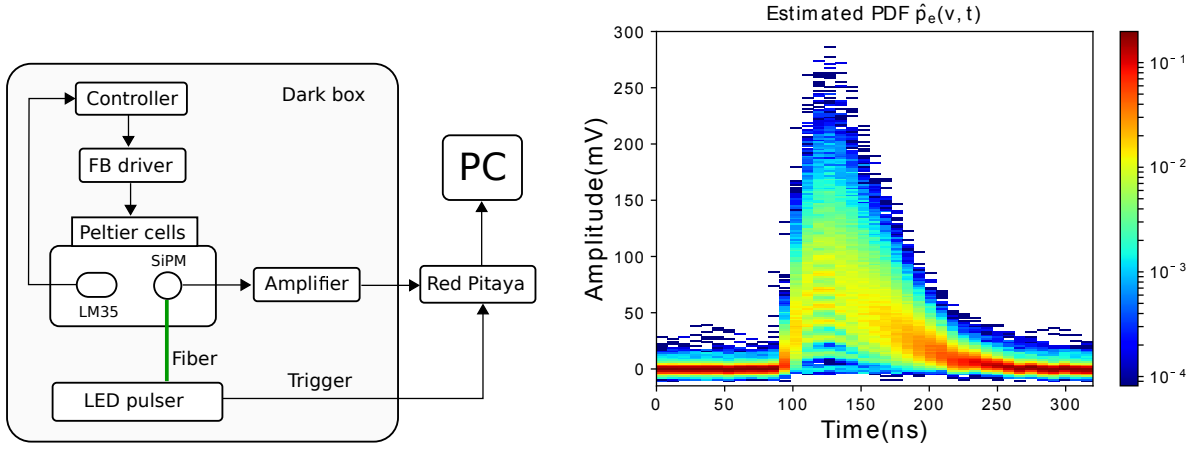


FIGURE 5: (Left) Experimental setup for measuring the gain and noise of the SiPM S13360-1350CS. A 480 nm pulsed light 10 ns width at 500 Hz stimulates the SiPM. The SiPM pulses are digitized at 14-bit/125 MHz. (Right) SiPM pulse waveform quantization.

We also performed a complete characterization of the signal attenuation along the scintillator strips [15]. We calibrated the hodoscope response using the atmospheric cosmic ray flux. It allows us also to determine the acceptance confidence window taking into account the variance of the measured open sky muon flux depending on the zenith angle. Figure 6 shows the muon number histogram after 15 hours of recording and the comparison between the estimated (red line) and measured (black points) muon flux. The measuring error increases with the zenith angle while the muon flux and the hodoscope acceptance decrease.

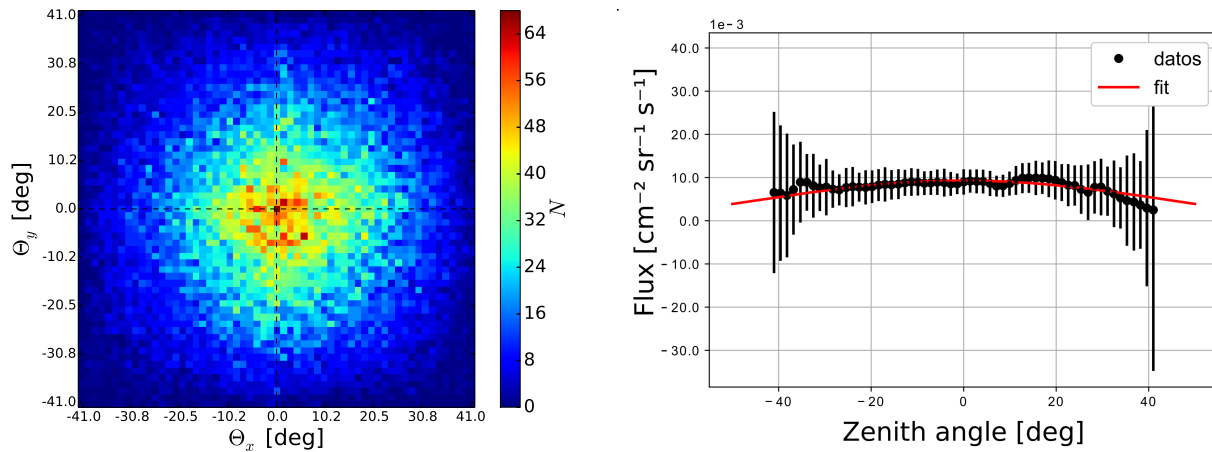


FIGURE 6: (Left) Particle count recorded by the hodoscope during 15 hours with a separation of 13 cm between panels. (Right) Open sky muon flux profile recorded by the hodoscope. The muon flux measurements (black line) range zenith angles between -40° and 40° . A \cos^n function fits the muon flux with $n \sim 2$.

5.1. Mechanics

We designed the detector mechanics and simulated its structural behavior under typical environmental conditions through SOLIDWORKS. We determined an average temperature of 23°C on the MuTe with maximum temperatures reaching $\sim 60^\circ\text{C}$ in the center of the scintillation panels due to solar radiation. The water volume ($\sim 1.7\text{ m}^3$) of the WCD and the wind flow reduce the telescope temperature.

The mechanical structure of MuTe was found to be robust against tremors and vibrations triggered by volcanic activity. The MuTe vibrations did not exceed 0.04 Hz, guaranteeing its structural integrity [20].

6. DATA ANALYSIS

The MuTe performed its first muogram after two months of data recording pointing toward the mountain range at the northwest of Bucaramanga-Colombia with an elevation of 15° . The open sky muon flux Φ_0 was estimated considering the data recorded during the hodoscope calibration stage. Figure 7 shows the MuTe view and the obtained muogram [34].

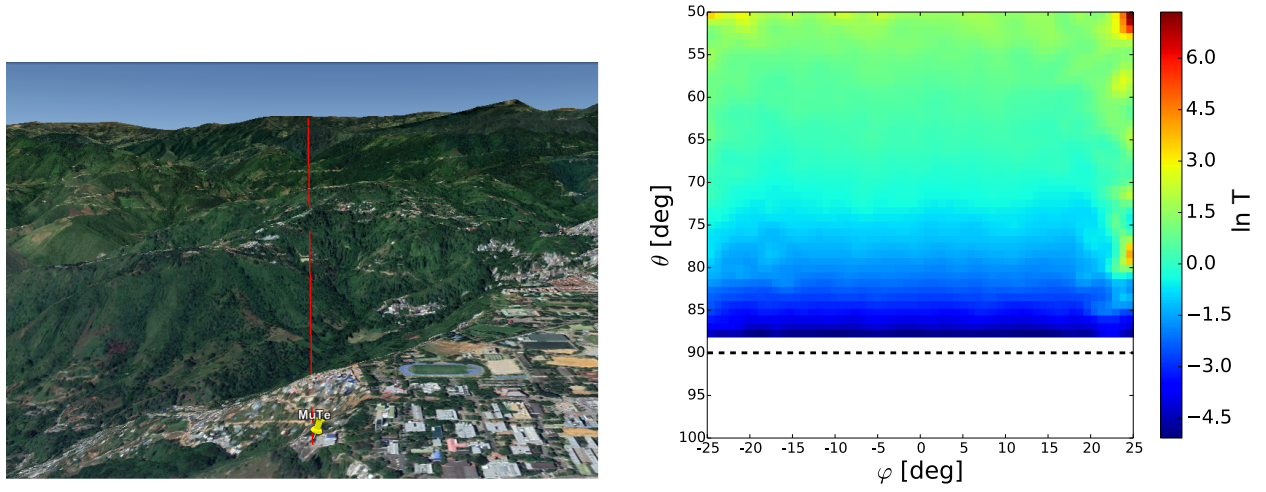


FIGURE 7: (Left) Frontal view of the mountain range scanned by the MuTe. The telescope has an elevation angle of $\sim 15^\circ$ covering zenith angles from 50° to 90° and 10° under the horizon. (Right) Muogram obtained by MuTe after 2-month data recording. The muogram is in terms of the logarithm of transmittance ($T = \ln \Phi / \Phi_0$) with Φ the emerging muon flux and Φ_0 open sky muon flux. In the open sky zones ($\Theta > 70^\circ$) $T \sim 1$ ($\ln T \sim 0$), while for the mountain region the transmittance decreases ($\ln T < 0$). Below the horizon line, the open sky flux is zero, and the transmittance is infinite.

6.1. Muography Background Characterization

MuTe data analysis allows us to understand the composition of particles impinging the detector during a muography acquisition run. Not only muons but also background particles impinge the detector. We found four background sources in muography: electromagnetic particles of extensive air showers (photons, electrons, and positrons), back-scattering particles, forward scattering muons, and multiple-particle events.

We characterized the muography background by analyzing the time of flight and deposited energy data. Electromagnetic background deposits an energy lower than 180 MeV and the multiple-particle component deposits an energy above 400 MeV with a significant contribution at 480 MeV (equivalent to 2 vertical muons) as shown in Figure 8(left).

Multiple-particle component splits in two: correlated particles ($\Delta t < 100$ ns) originated in the same shower and uncorrelated/independent particles ($\Delta t > 300$ ns) as shown in Figure 8(right).

The deposited energy information allows us to determine the particle mass. The incident particle momentum was estimated using the ToF measurements, the traversing distance, and the particle mass [23]. We set a threshold to reject muons with momentum below 1 GeV/c as shown in Figure 8.

We have implemented a machine learning algorithm to classify and reduce the muography background. Firstly, we train a Gaussian Mixture Model to parameterize the deposited energy spectrum and establish thresholds to separate the electromagnetic and multiple-particle background. Then, we use an algorithm to filter low momentum muons (< 1 GeV/c) by thresholding [35].

6.2. Density Inversion

A crucial step in muography data processing is to solve the inverse problem to determine the inner density distribution of the scanned target. We implemented the Metropolis-Simulated-Annealing algorithm, which inputs an observed muon flux and obtains the best-associated density distribution of the Cerro Machin volcano.

We simulated an inner structure of the Cerro Machín composed of a conduit below the volcano fumaroles zone as shown in Figure 9. We improved this model by including rock densities from samples taken from the crater, the dome, and the areas associated with fumaroles. The inversion algorithm reconstructed the density differences inside the emulated Cerro Machín structure from the measured muon flux within a 1% error. The result showed a remarkable density contrast between the volcanic duct, the encasing rock, and the fumarole area [18].

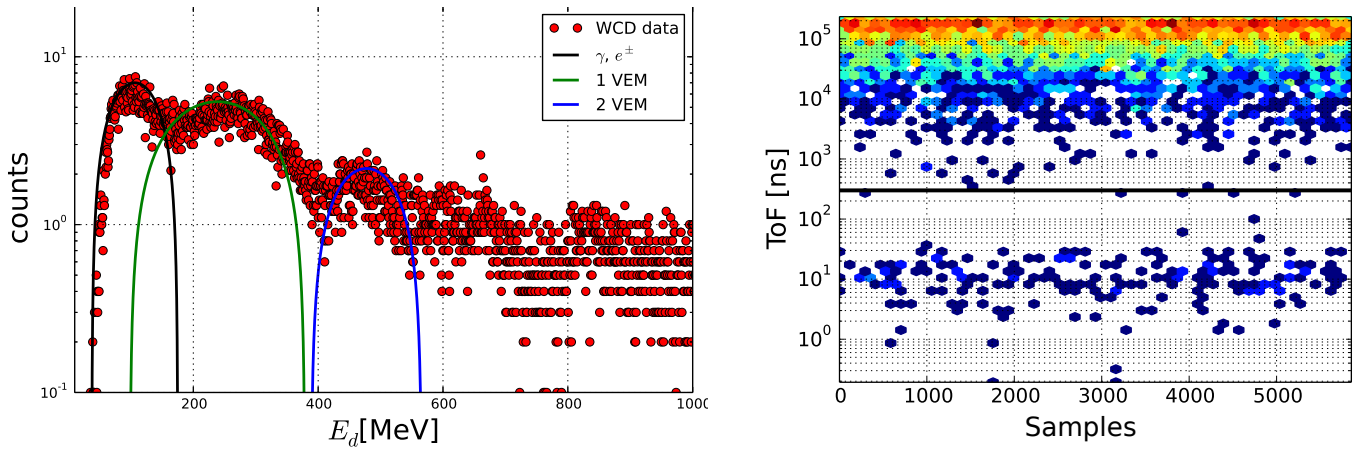


FIGURE 8: (Left) Deposited energy histogram for particles crossing the MuTe during one hour. The black-line hump (<180 MeV) corresponds to the electromagnetic component. The green-line hump (180 MeV $< E_d < 400$ MeV) indicates the deposited energy of muons. Multiple-particle events (blue line) deposit energy above 400 MeV. (Right) The time of flight of particles traversing the MuTe hodoscope. Single-particle events and correlated backgrounds have a ToF < 100 ns, while the uncorrelated background has a ToF > 300 ns.

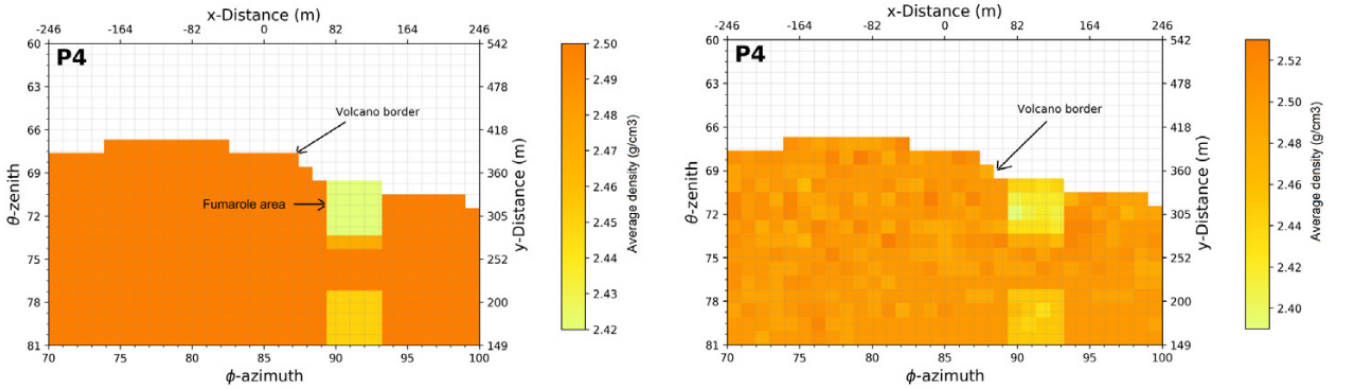


FIGURE 9: (Left) The synthetic density model of the Cerro Machin volcano. (Right) The profile after the inversion. The contrast of densities between the volcanic conduit and the surrounding rock remains [18].

7. DISCUSSION

The MuTe project plays a significant role in the muography development in Colombia, Argentina, and the Latin American region. We summarize our contributions from creating a simulation framework for muography, instrumentation implementations, and data analysis.

We simulated the physics behind the muography technique, the cosmic ray flux, the geomagnetic modulation, the creation of extensive air showers in the Earth's atmosphere, the muon flux passing through the geologic structure, the energy loss and scattering of muons, and the detector response. This model can be adapted to any geographical location and detector technology.

We designed a hybrid Muon Telescope combining a tracking system and a water Cherenkov detector. We can identify muography background sources, electromagnetic particles, back-scattering particles, forward scattering muons, and multiple-particle detection during the data analysis. Finally, we have separated the background components using the deposited energy, tracking, and momentum information. This approach allows us to get extra information about particles impinging the detector.

The MuTe project also addresses the inverse problem of estimating the density distribution of volcanoes. We solved the optimization problem using a simulated annealing algorithm. We reconstructed the inner structure of the emulated volcano with an error of 1%. The muography program of the Universidad Industrial de Santander offers a training research environment for the new generation of Colombian interdisciplinary particle scientists.

CONFLICTS OF INTEREST

The authors declare that there are no conflicts of interest regarding the publication of this paper.

ACKNOWLEDGMENTS

The authors recognize the financial support of Departamento Administrativo de Ciencia, Tecnología e Innovación de Colombia (ColCiencias) under contract FP44842-082-2015 and to the Programa de Cooperación Nivel II (PCB-II) MINCYT-CONICET-COLCIENCIAS 2015, under project CO/15/02. We are also very thankful to LAGO and the Pierre Auger collaborations for their continuous support.

References

- [1] C. R. Stern. Active andean volcanism: its geologic and tectonic setting. *Revista geológica de Chile*, 31(2), December 2004.
- [2] K. Reath, M. Pritchard, M. Poland, F. Delgado, S. Carn, D. Coppola, B. Andrews, S. K. Ebmeier, E. Rumpf, S. Henderson, S. Baker, P. Lundgren, R. Wright, J. Biggs, T. Lopez, C. Wauthier, S. Moruzzi, A. Alcott, R. Wessels, J. Griswold, S. Ogburn, S. Loughlin, F. Meyer, G. Vaughan, and M. Bagnardi. Thermal, deformation, and degassing remote sensing time series (CE 2000–2017) at the 47 most active volcanoes in latin america: Implications for volcanic systems. *Journal of Geophysical Research: Solid Earth*, 124(1):195–218, January 2019.
- [3] G. P. Cortés. Informe de actividad volcánica segmento norte de colombia diciembre de 2016. Technical report, INGEOMINAS, 2016.
- [4] A. Agudelo. Informe técnico de actividad de los volcanes nevado del Huila, Puracé y Sotará, durante el período de diciembre de 2016. Technical report, Servicio Geológico Colombiano, 2016.
- [5] E. Muñoz. Informe mensual de actividad de los volcanes Galeras, Cumbal, Chiles, Cerro Negro, Las Animas, Doña Juana y Azufra. Technical report, INGEOMINAS, 2017.
- [6] A. Vesga-Ramírez, D. Sierra-Porta, J. Peña-Rodríguez, J. D. Sanabria-Gómez, M. Valencia-Otero, C. Sarmiento-Cano, M. Suárez-Duraán, H. Asorey, and L. A. Núñez. Muon tomography sites for colombian volcanoes. *Annals of Geophysics*, 63(6), December 2020.
- [7] H. F. Murcia, M. F. Sheridan, J. L. Macías, and G. P. Cortés. TITAN2d simulations of pyroclastic flows at cerro machín volcano, colombia: Hazard implications. *Journal of South American Earth Sciences*, 29(2):161–170, March 2010.
- [8] S. De la Cruz-Reyna and A. L. Martin Del Pozzo. The 1982 eruption of el chichón volcano, mexico: Eyewitness of the disaster. *Geofísica Internacional*, 48(1), January 2009.
- [9] H. Asorey, R. Calderón-Ardila, C. R. Carvajal-Bohorquez, S. Hernández-Barajas, L. Martínez-Ramírez, A. Jaimes-Motta, F. León-Carreño, J. Peña-Rodríguez, J. Pisco-Guavabe, J. D. Sanabria-Gómez, M. Suárez-Durán, A. Vásquez-Ramírez, K. Forero-Gutiérrez, J. Salamanca-Coy, L. A. Núñez, and D. Sierra-Porta. Astroparticle projects at the eastern colombia region: facilities and instrumentation. *Scientia et Technica*, 23(3):391–396, 2018.
- [10] H. Asorey, R. Calderón-Ardila, K. Forero-Gutiérrez, L. A. Núñez, J. Peña-Rodríguez, J. Salamanca-Coy, J. D. Sanabria-Gómez, J. Sánchez-Villafrades, and D. Sierra-Porta. minimate: A muon telescope prototype for studying volcanic structures with cosmic ray flux. *Scientia et Technica*, 23(3):386–390, 2018.
- [11] H. Asorey, L. A. Núñez, and M. Suárez-Durán. Preliminary results from the latin american giant observatory space weather simulation chain. *Space Weather*, 16(5):461–475, May 2018.
- [12] J. Grisales-Casadiegos, C. Sarmiento-Cano, and L. A. Núñez. Impact of global data assimilation system atmospheric models on astroparticle showers. *arXiv preprint arXiv:2006.01224*, 2020.
- [13] A. Tapia, D. Dueñas, J. Rodríguez, J. Betancourt, and D. A. Martínez Caicedo. Preliminary monte carlo simulation study of the structure of the galeras volcano using muon tomography. In *Proceedings of 38th International Conference on High Energy Physics—PoS(ICHEP2016)*. Sissa Medialab, February 2017.
- [14] J. S. Useche Parra and C. A. Ávila Bernal. Estimation of cosmic-muon flux attenuation by monserrate hill in bogota. *Journal of Instrumentation*, 14(02):P02015–P02015, February 2019.
- [15] A. Vásquez-Ramírez, M. Suárez-Durán, A. Jaimes-Motta, R. Calderón-Ardila, J. Peña-Rodríguez, J. Sánchez-Villafrades, J. D. Sanabria-Gómez, H. Asorey, and L. A. Núñez. Simulated response of MuTe, a hybrid muon telescope. *Journal of Instrumentation*, 15(08):P08004–P08004, August 2020.
- [16] I. D. Guerrero, D. F. Cabrera, J. C. Paz, J. D. Estrada, C. A. Villota, E. A. Velasco, F. E. Fajardo, O. Rodriguez, J. Rodriguez, D. Arturo, D. Dueñas, D. Torres, J. Ramirez, J. Revelo, G. Ortega, D. Benavides, J. Betancourt, A. Tapia, and D. A. Martinez-Caicedo. Design and construction of a muon detector prototype for study the galeras volcano internal structure. *Journal of Physics: Conference Series*, 1247(1):012020, June 2019.
- [17] A. Menchaca-Rocha. Using cosmic muons to search for cavities in the pyramid of the sun, teotihuacan: preliminary results. In *Proceedings of 10th Latin American Symposium on Nuclear Physics and Applications—PoS(X LASNPA)*. Sissa Medialab, October 2014.
- [18] A. Vesga-Ramírez, J. D. Sanabria-Gómez, D. Sierra-Porta, L. Arana-Salinas, H. Asorey, V. A. Kudryavtsev, R. Calderón-Ardila, and L. A. Núñez. Simulated annealing for volcano muography. *Journal of South American Earth Sciences*, 109:103248, August 2021.
- [19] N. Lesparre, J. Marteau, Y. Déclais, D. Gibert, B. Carlus, F. Nicollin, and B. Kergosien. Design and operation of a field telescope for cosmic ray geophysical tomography. *Geoscientific Instrumentation, Methods and Data Systems*, 1(1):33–42, April 2012.
- [20] J. Peña-Rodríguez, J. Pisco-Guabave, D. Sierra-Porta, M. Suárez-Durán, M. Arenas-Flórez, L. M. Pérez-Archila, J. D. Sanabria-Gómez, H. Asorey, and L. A. Núñez. Design and construction of MuTe: a hybrid muon telescope to study colombian volcanoes. *Journal of Instrumentation*, 15(09):P09006–P09006, September 2020.
- [21] J. Peña-Rodríguez, A. Vásquez-Ramírez, J. D. Sanabria-Gómez, L. A. Nunez, D. Sierra-Porta, and H. Asorey. Calibration and first measurements of MuTe: a hybrid muon telescope for geological structures. In *Proceedings of 36th International Cosmic Ray Conference—PoS(ICRC2019)*. Sissa Medialab, July 2019.
- [22] R. Calderón Ardila, H. Asorey, and A. Almela. Desarrollo de técnicas de muografía para estudios densimétricos de objetos de importancia estratégica. *AJEA*, (5), October 2020.
- [23] J. Peña Rodríguez, R. de León Barrios, A. Ramírez-Muñoz, D. Villabona-Ardila, M. Suárez-Durán, A. Vásquez-Ramírez, H. Asorey, and L. A. Núñez. Muography background sources: simulation, characterization, and machine-learning rejection. In *Proceedings of 37th International Cosmic Ray Conference—PoS(ICRC2021)*. Sissa Medialab, August 2021.
- [24] N. Lesparre, D. Gibert, and J. Marteau. Bayesian dual inversion of experimental telescope acceptance and integrated flux for geophysical muon tomography. *Geophysical Journal International*, 188(2):490–497, November 2011.
- [25] H. Asorey, L. A. Núñez, M. Suárez-Durán, L. A. Torres-Niño, M. Rodríguez-Pascual, A. J. Rubio-Montero, and R. Mayo-García. The latin american giant observatory: a successful collaboration in latin america based on cosmic rays and computer science domains. In *Cluster, Cloud and Grid Computing (CCGrid), 2016 16th IEEE/ACM International Symposium on*, pages 707–711. IEEE, 2016.

- [26] C. Sarmiento-Cano, M. Suárez-Durán, R. Calderón-Ardila, A. Vásquez-Ramírez, A. Jaimes-Motta, S. Dasso, I. Sidelnik, L. A. Núñez, and H. Asorey. Performance of the LAGO water Cherenkov detectors to cosmic ray flux. *arXiv preprint arXiv:2010.14591*, 10 2020.
- [27] M. L. Valencia-Otero. Estudio de las componentes de secundarios en cascadas originadas por rayos cósmicos para aplicaciones sobre estructuras geológicas. Master's thesis, Universidad Industrial de Santander, 2016. Bachelor's Thesis.
- [28] V. A. Kudryavtsev. Muon simulation codes music and musun for underground physics. *Computer Physics Communications*, 180(3):339–346, 2009.
- [29] H. Moss, A. Vesga-Ramírez, V. A. Kudryavtsev, L. A. Núñez, and D. Sierra-Porta. Muon tomography for the cerro machín volcano. Technical report, Department of Physics & Astronomy, University of Sheffield, Sheffield, United Kingdom, 2018.
- [30] L. V. Girón-Lozano. Cálculo de pérdida de energía de muones que interactúan con diferentes tipos de roca: aplicación al volcán Cerro Machín para el proyecto MuTe, en el rango de energía de 1 a 1000 GeV. Master's thesis, Universidad del Tolima, 2020.
- [31] J. Peña Rodríguez. *Diseño y calibración de un telescopio de muones híbrido para estudios vulcanológicos*. PhD thesis, Universidad Industrial de Santander, 2021.
- [32] J. Sánchez-Villafrades, J. Peña Rodríguez, H. Asorey, and L. A. Núñez. Characterization and on-field performance of the MuTe Silicon Photo-multipliers. 2 2021.
- [33] J. Sánchez-Villafrades, J. Peña Rodríguez, R. Calderón-Ardila, and L. A. Núñez. Control de temperatura para el estudio del voltaje de ruptura de SiPMs. In *Congreso Internacional de Ciencias Básicas e Ingeniería—(CICI2018)*. Universidad de los Llanos, August 2018.
- [34] L. A. Nunez, R. de Leon-Barrios, J. Peña-Rodríguez, J. D. Sanabria-Gómez, A. Vásquez-Ramírez, R. Calderón-Ardila, C. Sarmiento-Cano, A. Vesga-Ramirez, D. Sierra-Porta, M. Suárez-Durán, and H. Asorey. Muography for the colombian volcanoes. In *Proceedings of 37th International Cosmic Ray Conference—PoS(ICRC2021)*. Sissa Medialab, August 2021.
- [35] A. Ramírez-Muñoz and D. Villabona-Ardila. Discriminación del ruido de fondo en muografía usando técnicas de aprendizaje automatizado. Master's thesis, Universidad Industrial de Santander, 2021. Bachelor's Thesis.